

METHODOLOGY FOR A PLANCK/HERSCHEL ANALYSIS OF THE INTERPLAY BETWEEN FILAMENTS AND MAGNETIC FIELDS IN STAR FORMING REGIONS

J.-S. Carrière¹, L. Montier¹, I. Ristorcelli¹ and K. Ferrière¹

Abstract.

Interstellar matter in star forming regions appears to form filamentary structures, which were suggested to line up either parallel or perpendicular to the magnetic field. Our purpose is to investigate this possible alignment further, based on a combined analysis of Herschel and Planck data obtained towards a large variety of star forming regions. As a first step, we developed an optimized version of the original Rolling Hough Transform code, particularly well suited to extract and analyse the orientation of filamentary structures over a broad range of densities, from striations to dense filaments. In this paper, we present an overview of our new method, called the Rolling Radon Transform and we describe the preliminary results obtained for a star forming region at high galactic latitude.

Keywords: Star formation, ISM, Magnetic field, Polarization

1 Introduction

Magnetic fields are considered as one of the key physical agents, with gravitation and turbulence, that regulate star formation, but their actual role in the formation and evolution of dense structures remains an open question. Thanks to the capability of alignment of elongated grain on magnetic fields, polarized dust emission is well-suited to probe the magnetic field structure in the cold, dense interstellar medium (ISM).

Exploring the submillimeter domain with unprecedented performances in terms of sensitivity, sky coverage and angular resolution, the complementary between the Planck and Herschel satellites has opened a new era for the study of the cold matter structures in the Galaxy. Thousands of cold cores and clumps have been detected in different Galactic environments (Planck Collaboration et al. 2016c), and the surveys have revealed a network of filamentary structures, ubiquitous over a wide range of physical conditions. Moreover, it was shown that prestellar cores and protostars form primarily within the densest filaments (André et al. 2010). Therefore, the question of the formation of prestellar cores is now closely linked to the properties of filaments, their formation, and their evolution.

The study of the relative alignment between filaments hosting cold cores and magnetic fields in star forming regions offers a unique opportunity to investigate the possible link between them. Recent studies revealed preferential relative orientations, varying from parallel in the diffuse medium (Planck Collaboration et al. 2016a) to perpendicular in denser filaments within the molecular clouds (Planck Collaboration et al. 2016b). A transition in column density between parallel and perpendicular configurations was found and shown to be consistent with simulations assuming strong magnetic fields (Planck Collaboration et al. 2016b). In a statistical analysis of a sample of filaments hosting clumps, Alina et al. (2019) found that the relative orientations (parallel, perpendicular or no preference) depended both on the environment density and on the density gradient between the filaments and their environment.

In order to gain more insight in the interplay between filaments and the magnetic field, Malinen et al. (2016) performed for the first time a combined analysis of Planck and Herschel data toward the star forming region L1642 (also called G210 here). Comparing the magnetic field traced by the dust polarized emission observed by Planck and the highly resolved matter structures observed by Herschel will give us more detailed information on the relative alignment study. Especially for the less dense filaments, called striations, that were not resolved in

¹ CNRS, IRAP, 9 Av. colonel Roche, BP 44346, 31028 Toulouse Cedex 04, France

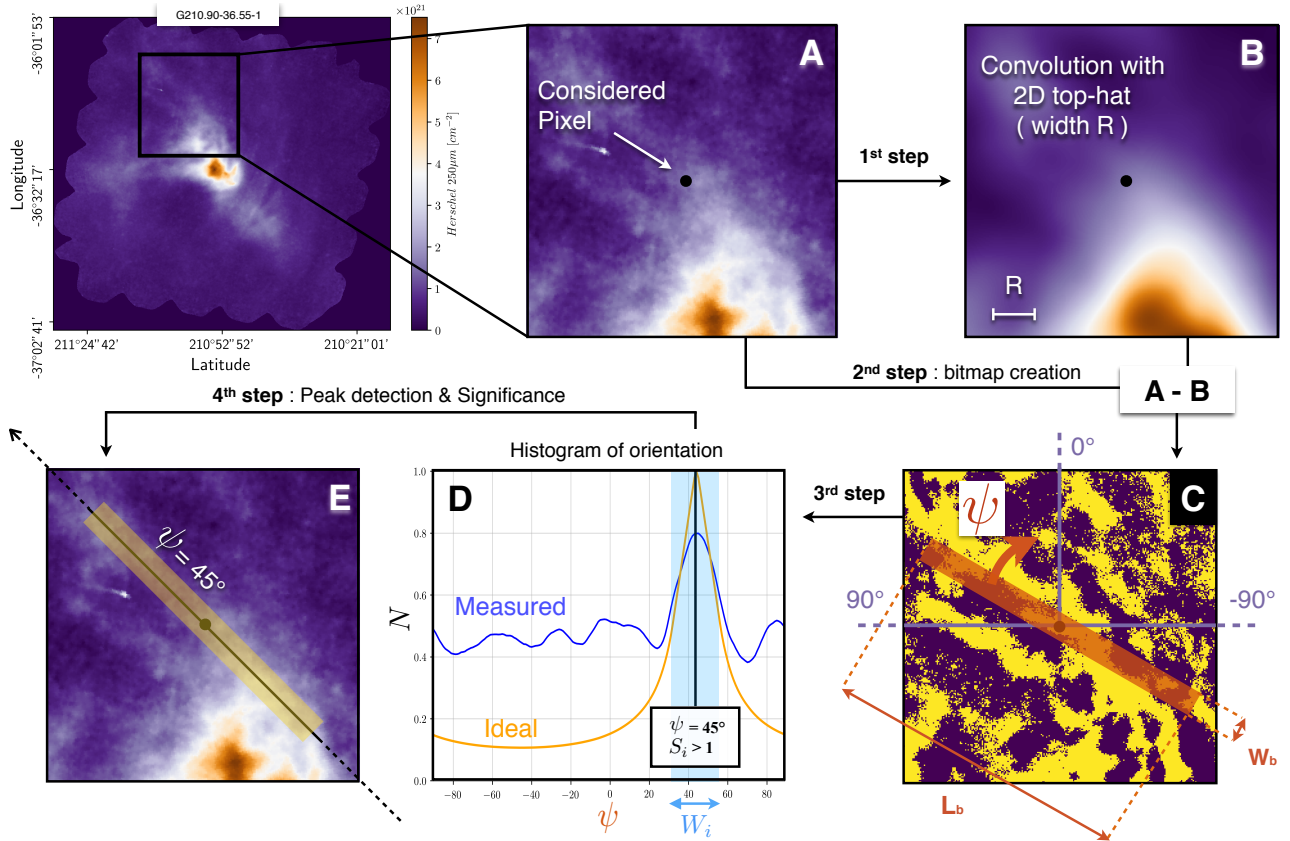


Fig. 1. Illustration of the RRT method based on the 250 μm intensity map of the G210 field observed by Herschel. **Top Left:** Entire G210 field. **Top Middle:** Region A from this field. **Top Right:** Smoothed image B from the initial image A obtained by convolving with a 2D top-hat kernel. **Bottom Right:** Binary image C in which the dark pixels have a value of 0 and the yellow pixels, which represent the sharpest structures from the initial image A, have a value of 1. **Bottom Middle:** The correlation between the nominal bar and the yellow pixels in the binary image is shown in the Histogram of orientation D. **Bottom Left:** Detected filament in the image E (with the initial image A as background) around the initial pixel considered with the orientation found in the Histogram of orientation D.

Planck data. They found a very similar transition as in Planck Collaboration et al. (2016b) in terms of column density ($N_{\text{H}} \approx 1.7 \times 10^{21} \text{ cm}^{-2}$), and noted that diffuse filaments (called striations) are clearly parallel to the magnetic field. G210 is part of the sample of 116 selected fields from the Herschel "Galactic Cold Cores" key-program (Juvela et al. 2012), a follow-up of the Planck Galactic Cold Clumps catalogue (Planck Collaboration et al. 2016c), put together to study star formation in different Galactic environments.

Our ultimate goal is to perform a similar analysis as in Malinen et al. (2016) extended to this whole fields sample. For that purpose, we first developed an improved methodology to extract filaments, especially useful in the case of a statistical analysis (Carrière et al. in prep). Here we present the main steps of this method, called the Rolling Radon Transform (RRT), which is an optimization of the Rolling Hough Transform (RHT) method (Clark et al. 2014). We also present the preliminary results derived when applying this new method to the G210 field.

2 Rolling Radon Transform Methodology

Binary map

The new RRT method is illustrated in Fig. 1, applied to one pixel from the G210 field. As for the RHT, the first step of the RRT method is to create a smoothed image B from the initial image A, by convolving A with a 2D Top-hat function of radius R. The subtraction of A by B gives C in which the negative pixels obtain the

value zero and the positive pixels, representing the sharpest structures in A, obtain the value of 1. The value of R is a free parameter in RHT and thus is not taking into account the sharp structures size from C as a function of the nominal bar's width. This can lead to misunderstanding in the final output since those sharp structures should have sizes the closest possible to the nominal bar's width. This is now optimized in the RRT and the processing method will be described in Carrière et al. in prep.

Histogram of orientation

Both RHT and RRT methods are based on the approximation that filaments can be considered as bars with lengths L_b and widths W_b . The second step of both methods is to compute the correlation between this nominal bar and the binary image for any main axis bar's orientation ψ , in the range -90° to $+90^\circ$. This provides a "measured" histogram against orientation (panel D in Fig. 1). This histogram thus gives the fraction N of the bar surface that is yellow.

From this histogram of orientation, the RHT uses two important assumptions. The first one is to apply a threshold N_{ct} on N and consider the filament's orientation as the mean value of the angles ψ in the histogram part that is higher than N_{ct} . The second assumption of the RHT is to consider that this free parameter N_{ct} is sufficient to quantify the reliability of the extracted filaments. For the first assumption, an important issue may occur when we have two different peaks at two different positions (in terms of angle) that are higher than N_{ct} in the histogram of orientation. Indeed, in that case, the mean value of the angles ψ will give a wrong filament's orientation between the two different peaks and miss the fact that both peaks eventually correspond to two different filaments with two different orientations. For the second assumption, it is clear that this free parameter N_{ct} is intrinsic to the method and can be arbitrary. Those two assumptions are removed in the RRT and the filament's orientation and its reliability computation are now optimized. We will now focus in more details on the new RRT methodology.

The first optimization is to compute the orange curve of panel D that represents an ideal histogram as would be obtained if the binary image contained a single yellow region with the exact same shape as the nominal bar. Thus, it shows a peak at a given angle, corresponding to the preferential orientation maximising the correlation between the bar and the structures in the binary image.

Significance

We will consider each peak in the measured histogram as a potential filament with its own orientation. For each peak, we consider the ideal histogram that peaks at the same position that we compare with the measured histogram over a window W_i of orientation angles related to the bar's dimension. The comparison is done by calculating the parameter Δ as follows,

$$\Delta = \sqrt{\frac{\chi^2}{n}} = \sqrt{\frac{1}{n} \times \sum_j^n \frac{(I_j - M_j)^2}{\sigma^2}}, \quad (2.1)$$

$$\sigma = \text{MAD} = \text{median}(|M - \text{median}(M)|), \quad (2.2)$$

with n the number of considered points within the comparison window W_i , M the measured histogram, I the ideal histogram and MAD the mean absolute deviation. The next step is to decide whether a detected structure is a reliable filament or not, thus we have to define a threshold Δ_{ct} on Δ . To define a non-arbitrary threshold, we perform Monte-Carlo simulation. We can see in Fig. 2 an illustration of one Monte Carlo step. The idea is to add the RRT bar inside the field binary image, with random position and orientation. The only difference between the measured and ideal histograms is that the measured includes the field background.

The following step is to repeat this process at least ten thousand times (with random positions and orientations for the bar) in order to obtain a Δ distribution. This distribution allows us to define a threshold Δ_{ct} that is directly linked to the field background and thus specific to each field. The computation of Δ_{ct} is based on a p-value of 5%. Let's assume we have a realization Δ_{ct} of a random variable Δ following the distribution D , then

$$p := \text{Pr}(\Delta > \Delta_{ct} | D), \quad (2.3)$$

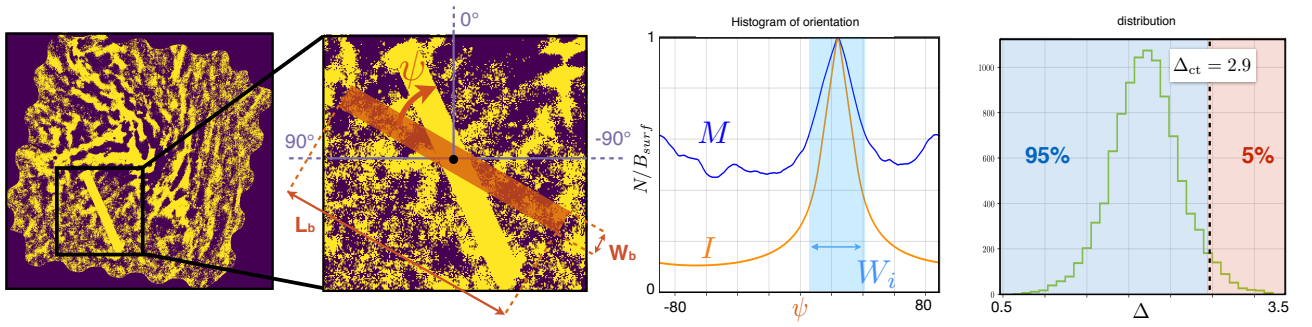


Fig. 2. Left & Middle Left: Binary image of the G210.90-36.55-1 field in which we add a bar with random position and orientation and with the exact same shape as the standard RRT bar. **Middle Right:** Resulting measured and ideal histograms of orientation. **Right:** Δ distribution (Monte-Carlo simulation) with the threshold Δ_{ct} by considering a p-value of 5%.

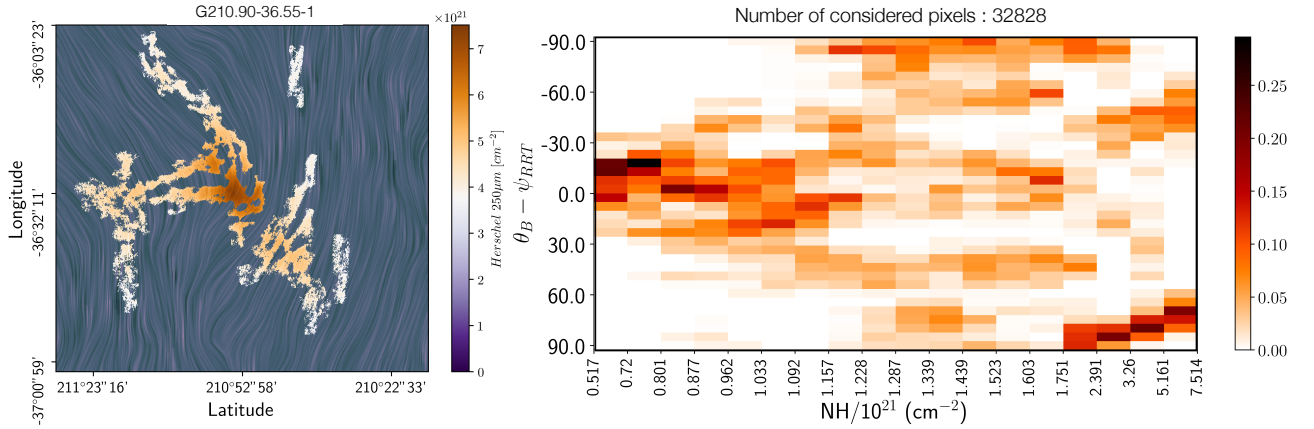


Fig. 3. Left: Filaments extracted with the RRT, with the magnetic field traced by the dust polarized emission of G210. **Right:** Histogram of Relative Orientation $\theta_B - \psi_{RRT}$ as function of column density N_H .

with p the probability that Δ is larger than Δ_{ct} assuming the distribution D . We can see in Fig. 2 the value of the resulting threshold Δ_{ct} given a p-value of 5%. If we want to have something comparable between the different fields, we will consider a significance S_i given by $S_i = \Delta_{ct}/\Delta$. This equation tells us that the significance is > 1 if Δ is lower (thus better) than the threshold Δ_{ct} and vice versa. Finally, a significance > 1 means that the filament detected by the RRT is a reliable filament and its parameters, such as its orientation, will be kept for science analysis. In view of the definition of the p-value, this means we have a 5% chance of rejecting the ideal filament that we were looking for (by considering filaments as bars).

Compared to the two assumptions made by RHT, one of the main advantages of the RRT method is now the possible detection of different filamentary structures, without bias between each others, with different orientations for one pixel of the field. The second optimization is about the significance S_i that gives us a statistical, non-arbitrary and thus robust computation of the filament extraction reliability.

3 Preliminary results

Once we have extracted the orientation of filaments in a reliable way with the RRT, we can study their relative alignment with respect to the magnetic field whose orientation θ_B is based on polarization data measured by Planck. In order to illustrate these preliminary results, we use the example of the G210 field for which we apply the RRT with $L_b=0.1\text{pc}$ and $W_b=0.3\text{pc}$. These width and length come from Arzoumanian et al. (2019) who found a characteristic filament width of 0.1pc by imposing an aspect ratio ≥ 3 . In Fig. 3 we can see the combination of the filaments detected by the RRT with the magnetic field traced by the dust polarized emission.

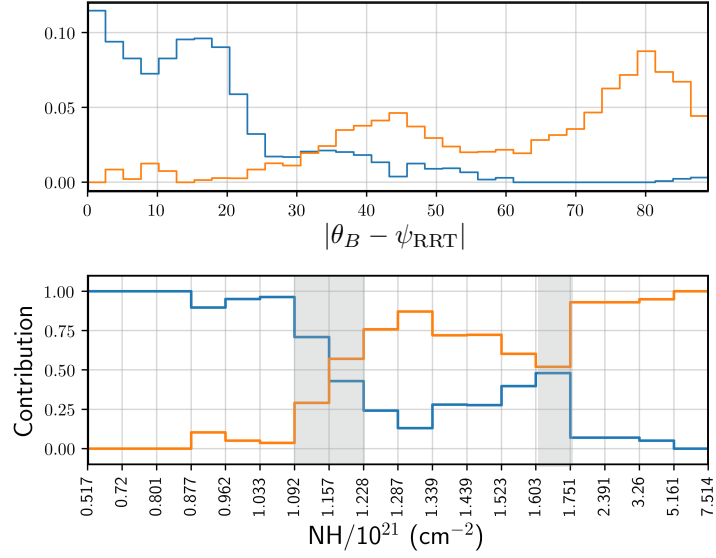


Fig. 4. Top: HROs integrated over all N_{H} for the two main components emerging from Resulting main components from Fig 3, Right. **Bottom:** Weights of these two components as functions of column density.

We first show (Fig. 3, Right) the Histogram of Relative Orientation (HRO) $\theta_B - \psi_{\text{RRT}}$ as a function of column density N_{H} . We can clearly see that, on the left part, at lower densities, the less dense filaments are mainly aligned parallel to the magnetic field, while they tend to be perpendicular at higher column density. This result is very consistent with the previous study of Malinen et al. (2016).

We use the Principal Component Analysis (PCA) and the Non-negative Matrix Factorization (NMF). The aim of using these two methods is to reconstruct the HRO vs N_{H} diagram as two different matrices representing the principal components H and their weights W as explained in Malinen et al. (2016). As we can see in Fig. 4, we obtain two main components from H that can reconstruct the HRO vs N_{H} diagram, thus a bimodal orientation. Here we find that the transition column density between the two modes is about $1.2 \times 10^{21} \text{ cm}^{-2}$. However, we also notice a region around $1.7 \times 10^{21} \text{ cm}^{-2}$ without a clear distinction between the two components, where both weights are about 50%. This is close to the value found in Malinen et al. (2016) and Planck Collaboration et al. (2016b), and the reason this is not a transition in our case may come from the difference between the methods used in order to extract the filaments.

4 Conclusion

Our new RRT method provides a very robust way of extracting filaments with different sizes and in different environments, over a broad range of densities. Compared to the RHT, we improved the computation of the extracted filament significance, now based on a statistical study rather than on arbitrary parameters. It is user friendly (the only parameters to control are the bar dimensions) and relatively fast (less than 30 minutes per molecular cloud), which is a great asset for the statistical analysis that we plan to do in the future on all the 116 fields from Herschel PGCC follow-up. It is clear that combining Herschel and Planck data is quite powerful for the relative alignment study since it includes striation features, thinner structures than filaments in molecular clouds that Planck alone can't resolved. We also found a bimodal orientation between filaments and the magnetic field. This result, on G210 field, is part of a preliminary study carried on a sample of different fields studied by Alina et al. (2019) (Carrière et al. in prep).

References

- Alina, D., Ristorcelli, I., Montier, L., et al. 2019, MNRAS, 485, 2825
 André, P., Men'shchikov, A., Bontemps, S., et al. 2010, A&A, 518, L102
 Arzoumanian, D., André, P., Könyves, V., et al. 2019, A&A, 621, A42
 Clark, S. E., Peek, J. E. G., & Putman, M. E. 2014, ApJ, 789, 82

- Juvela, M., Pelkonen, V. M., White, G. J., et al. 2012, *A&A*, 544, A14
- Malinen, J., Montier, L., Montillaud, J., et al. 2016, *MNRAS*, 460, 1934
- Planck Collaboration, Adam, R., Ade, P. A. R., et al. 2016a, *A&A*, 586, A135
- Planck Collaboration, Ade, P. A. R., Aghanim, N., et al. 2016b, *A&A*, 586, A138
- Planck Collaboration, Ade, P. A. R., Aghanim, N., et al. 2016c, *A&A*, 594, A28